**Post-Print**

This is the accepted version of:

A. Tamer, V. Muscarello, P. Masarati, G. Quaranta
*Evaluation of Vibration Reduction Devices for Helicopter Ride Quality Improvement*
Aerospace Science and Technology, Vol. 95, 105456, 2019, p. 1-11
doi:10.1016/j.ast.2019.105456

# EVALUATION OF VIBRATION REDUCTION DEVICES FOR HELICOPTER RIDE QUALITY IMPROVEMENT

Aykut Tamer[a,*], Vincenzo Muscarello[a], Pierangelo Masarati[a], Giuseppe Quaranta[a]

[a]*Dipartimento di Scienze e Tecnologie Aerospaziali, Politecnico di Milano, 20156-Milano/IT*

**Abstract**

This work presents the use of a modern helicopter simulation environment for the evaluation of the combined performance of several systems for helicopter ride quality assessment. The proposed framework can handle increasingly detailed aeroservoelastic helicopter models while providing great flexibility and versatility in modeling human biodynamic models for vibration evaluation as well as models of the vibration attenuation devices. A numerical model representative of a medium weight helicopter is used to demonstrate the approach. Lumped parameter models of seat-cushion and human biodynamics are dynamically coupled to the helicopter model to provide a more realistic estimate of the actual vibratory level experienced by the occupants. Two performance indicators are formulated, based on the acceleration of the seat locations and using the ISO-2631 standard: i) qualitative criteria and related vibration dose values of the individuals seated at prescribed locations of a fully occupied helicopter, and ii) an overall rating of the occupants inside the cabin, considering the most and least comfortable seating distributions as the number of occupants changes. To demonstrate the proposed method, three configurations of helicopter-specific passive vibration absorbers are considered.

*Corresponding author

*Email addresses:* `aykut.tamer@polimi.it` (Aykut Tamer), `vincenzo.muscarello@polimi.it` (Vincenzo Muscarello), `pierangelo.masarati@polimi.it` (Pierangelo Masarati), `giuseppe.quaranta@polimi.it` (Giuseppe Quaranta)

*Keywords:* helicopter ride quality, whole-body vibration, vibration reduction, transport ergonomics

## 1. Introduction

In helicopters, vibrations reduce the ride quality experienced by occupants and may cause chronic pain in the long-term [1]. A typical solution to improve ride quality is to design for the lowest possible vibration level, and add vibration attenuation devices when the goal cannot be achieved.

### *1.1. Helicopter Vibrations and Methods of Reduction*

Owing to the complex nature of the rotor blade-airflow interaction of rotary wing aircraft, vibration levels are higher in helicopters than in fixed-wing aircraft [2]. In the most broadly diffused helicopter configuration, the predominant vibratory loads originate from the main rotor, i.e. the larger size rotor located on top of the airframe. A rotor with equally spaced, identical blades acts as a filter when all the blade loads are summed in the non-rotating reference frame. As a result, only the loads at frequencies which are integer multiples of the rotor fundamental frequency $\Omega$ times the blade number $N_b$ ($N_b\Omega$, or $N_b$/rev in non-dimensional form) are transmitted to the fuselage [3]. When blades accidentally differ, severe vibrations at the rotor passing frequency, $\Omega$, might also occur, which can be minimized by balancing the rotor. However, $N_b$/rev vibrations and their multiples intrinsically exist regardless of the rotor balance condition and are dominant over other vibration sources, thus main rotor loads at $N_b$/rev can be considered as the main parameter for ride comfort assessment [4]. The amplitude of multiple harmonics is usually much lower, and occupants are less sensitive to higher frequencies, therefore have not primary importance. Other sources (wake interaction during descent flight, gust loads, etc.) can have significant consequences in terms of short interval discomfort, safety and piloting qualities, but act for a much shorter duration as compared to $N_b$/rev loads, which persist for the duration of translational flight; thus, the former are assumed to have limited impact on ride quality.

Despite the improvements in design technologies for reduced vibration, such as optimization techniques coupled to advanced simulation tools, it should not be surprising that the implementation of vibration attenuation devices is still standard practice in the rotorcraft industry [5]. To increase the occupants' comfort, it is worth considering any possible means of vibration attenuation, as long as proven airworthy. Many products, based on different technologies, are available for local vibration isolation of occupants. A complete review of possible means of vibration reduction is outside the scope of this work; therefore, we focus on helicopter-specific applications.

Vibration attenuation solutions can be classified as passive, active or semi-active. Passive solutions do not require any actuation; they aim at mechanically isolating the critical components. Such devices may be dedicated to broadband vibration reduction, or can be optimized for tonal vibration attenuation, when specifically tuned for a prescribed frequency. Whereas broadband passive attenuation devices are usually marginally effective for rotorcraft, tonal attenuation is very interesting, since a predominant source of vibration mainly acts at the previously mentioned $N_b$/rev frequency. A classical method benefits from mechanical amplification of the motion of a beater mass by means of a lever. One example is the DAVI (Dynamic Anti-resonant Vibration Isolator), which can be mounted in parallel to the gearbox suspension [6, 7]. A device that is similar in the operating concept is the ARIS (Anti-Resonance Isolation System), with mechanical and hydraulic versions [8]. An alternative design, whose beater is located in series with the gearbox suspension, is the SARIB (*Suspension Anti-Résonante Intégrée à Barres*, or anti-resonance suspension integrated with the struts) [9]. A different technique consists in accelerating a low viscosity fluid between two chambers and letting the pressure differential caused by the relative motion counteract the vibratory load [10, 11, 12]. The LIVE, or Fluidlastic[1], is an example of this concept [13]. In the rotating frame, pendulum absorbers attached on the blades [14] and rotor-head vibration absorbers [15] are two proven examples. Also for the human-airframe interface passive solutions are used; recently, seat cushion designs have been revisited for the comfort of the crew [16].

On the other hand, active techniques, which consume power, are implemented through on-board computers and servo actuators [17]. The goal is to generate counteracting oscillatory loads. Active vibration control at the rotor, i.e. at the source, is very common. An example is Higher Harmonic Control (HHC) [18, 19] of rotor blade pitch, in which the swash-plate is excited at higher harmonics and the corresponding motion is superimposed to the 1/rev collective and cyclic commands. The independent change of the pitch of each

[1]Fluidlastic™ is a trademark of Lord Corporation, Inc.

blade is referred to as Individual Blade Control (IBC) [20, 21, 22, 23]. Active isolation is also implemented by replacing the conventional gearbox struts with hydraulic actuators, as in the Active Control of Structural Response (ACSR) [17].

Semi-active techniques represent a trade-off between passive and active solutions. In this case, the device is adapted to changes in the excitation frequency by adjusting the passive mechanical properties using an actuator. However, the semi-active and passive devices can only store or dissipate energy, thus both follow exactly the same working principle [24]. An example is the self-tuning version of above-mentioned SARIB, having a tuning mass with adjustable moment arm with respect to the attachment point, to achieve anti-resonant operating conditions at different frequencies [25].

### *1.2. Comfort Assessment Standards*

Excitation arising from the contact surfaces cause the occupants' bodies to react, which is referred to as whole body vibration. The effectiveness of the aforementioned vibration reduction devices depends on the proper evaluation of whole body vibration, including its interaction with the excitation source. Standards have been devised to guide comfort assessment: the rather general ISO-2631 [26], the air vehicle specific NASA Ride Quality (RQ) [27], and the rotorcraft specific Intrusion Index (II) from Aircraft Design Standard (ADS) 27-A [28] deserve a mention. ISO-2631 operates on time domain accelerations at several vibration interfaces; it applies frequency weights with a qualitative scale. The RQ model uses the user-defined peaks of random or sinusoidal vibrations at the floor. The II is a frequency-domain method developed for highly periodic systems, which considers vibrations at the seat surface. Recent application of such standards to rotorcraft vibration problems include the evaluation of seat cushion designs for flight engineer seats [16] and the analysis of neck strain for different flights and pilot helmet configurations [29].

In Ref. [4], these standards were used for helicopter ride quality. It was concluded that the classical ISO-2631 better reflects the helicopter crew ratings than II or RQ. Starting from the discussion therein, the present work considers ISO-2631 as the framework for ride quality and revisits its critical aspects with regard to the characteristics of rotorcraft vibrations, applying it to the $N_b$/rev frequency.

*1.3. Perception of Vibration*

The sole acceleration measurements at locations of the airframe may be misleading when comfort or health of human subjects are considered, since the vibration level and its perception are not equivalent. The perception depends both on the frequency of the excitation and the body part that receives the excitations. Frequency weighting is a function that multiples a nominal vibration amplitude and converts it to an equal perception level at a given frequency to consider the human body sensitivity to the frequency of excitation rather than the mechanical characteristics of the vibrating surface [30]. Figure 1 presents the ISO-2631 version of human vibration sensitivity; the shaded area indicates a typical range of $N_b$/rev frequencies, which typically changes from 10 Hz to 30 Hz, with exceptional values as high as 47 Hz and as low as 4 Hz [5]. The plots present the frequency-dependent weights for the directional acceleration at the seat surface ($W_k$ and $W_d$), the acceleration of seat back ($W_c$), the motion sickness ($W_f$), the body rotation ($W_e$), and the recumbent person's head ($W_j$). All these curves behave similarly, showing a peak within a specific frequency bandwidth; however, they differ with respect to the location and range of that bandwidth. Within the typical $N_b$/rev frequency range, the sensitivity of a seated human ($W_k$, $W_d$, $W_c$ and $W_e$) to translational and rotational vibrations reduces significantly. Specifically, the amplitude of the vertical vibration weighting curve ($W_k$) is much larger than that of the lateral and longitudinal curves ($W_d$). Considering that the vertical hub loads are also greater in magnitude, the rotorcraft ride quality, excluding very specific designs and missions, is a problem of reducing the effect of vertical loads on the vertical vibrations of the human body, while trying not to amplify the accelerations in longitudinal and lateral directions. An exception is represented by Helicopter Emergency Medical Service (HEMS) missions, since typical values of $N_b$/rev lay in the frequency range of highest sensitivity for a recumbent person ($W_j$).

Vibration perception is also affected by the contact surface where excitation is transferred to the human body. This is addressed in ISO-2631 as multiplying factors to seat surface, back-rest, and feet acceleration components, in the three directions. The values of the coefficients, determined by the posture of the person, are reported in Table 1. The proposed method is able to implement all of these factors. Without loss in generality, this work focuses on seated subjects for illustrative purposes, due to the availability of seat-cushion data and biodynamic models of seated persons.

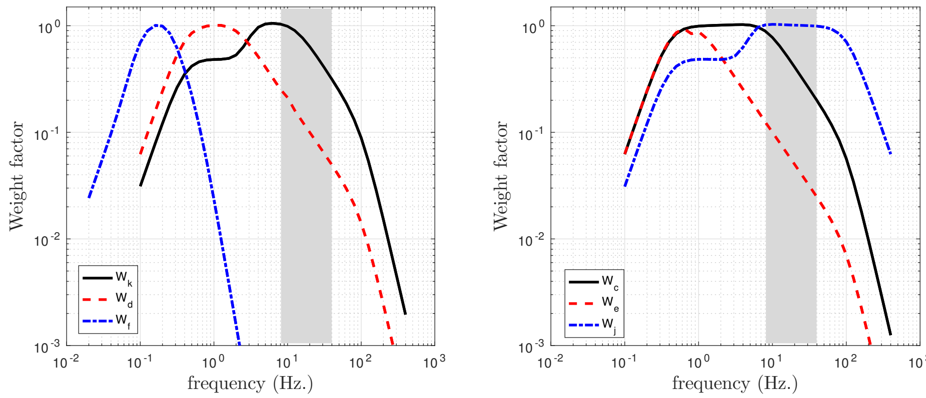


Figure 1: Weighting factors of ISO-2631 standard with typical helicopter $N_b$/rev frequency range shaded. $W_k$: seat-surface vertical direction, $W_d$: seat-surface horizontal and lateral directions, $W_f$: motion sickness, $W_c$: seat-back, $W_e$: rotational, $W_j$: head of a recumbent person.

Table 1: ISO 2631-1 Vibration perception multiplying factors of human body along frontal ($x$), transverse ($y$) and longitudinal ($z$) axes.

| Posture | Location | $k_x$ | $k_y$ | $k_z$ |
|---|---|---|---|---|
| Seating | Seat surface | 1.00 | 1.00 | 1.00 |
| | Back rest | 0.80 | 0.50 | 0.40 |
| | Feet | 0.25 | 0.25 | 0.40 |
| Standing | floor | 1.00 | 1.00 | 1.00 |
| Recumbent | floor | 1.00 | 1.00 | 1.00 |

### *1.4. Scope*

Evaluating the effectiveness of vibration reduction solutions requires a common environment to analyze increasingly complex vibration devices. A modular aeroservoelastic analysis framework that can collect sub-components (such as elastic airframe, rotor blades and human biodynamics models, vibration solutions etc.) modeled according to their most specific techniques is essential for the efficient modelling of the resulting assembly. To the authors' knowledge, the helicopter industry does not yet benefit from a tool of this sort when one or several vibration attenuation devices need to be optimized for human comfort.

The present paper addresses this need by presenting an original approach for performance evaluation of vibration reduction devices aimed at improving helicopter ride quality and illustrating its usefulness. The method is explained in Section 2. The development of a virtual helicopter environment is illustrated in Section 3, using realistic models of standard vibration absorption devices, combined with the effect of vehicle-human interaction. Two types of rotorcraft-specific vibration absorbers are selected for this purpose, although it should be emphasized that a broad variety of vibration reduction solutions can be successfully handled within the proposed framework. The numerical results are discussed in Section 4.

## 2. Method

Designing vibration absorbers to increase the ride quality of rotorcraft is a multi-objective design problem with tight constraints. First, the selection of the objective of the vibration attenuation is itself non-trivial, since many locations distributed within the cabin suffer from vibrations such as pilot and passenger seats. Besides, an airframe possesses multiple load paths and therefore many means of vibration suppression may need to cooperate. Moreover, some vibration absorbers attenuate vibrations at the design frequency and at a prescribed location. However, at some other frequency or spatial location, they can perform in a non-optimal way and may even amplify vibrations. Hence, a vibration engineer should be able to consider, and possibly affect, the design of all other components using a common platform. Last but not least, the outputs should be processed for a proper vibration index formulation, including the human perception of vibrations. These constraints require a large deal of experimental work, that could be significantly reduced through the adoption of a modular high-fidelity simulation environment.

### *2.1. Rotorcraft Modeling Environment*

Developed at Politecnico di Milano, MASST (Modern Aeroservoelastic State Space Tools) analyzes compact and complete linearized aeroservoelastic systems [31, 32]. In MASST, rotorcraft subcomponents are collected from well-known, reliable and state-of-the-art sources, and cast into state-space form using the Craig-Bampton Component Mode Synthesis (CMS) [33]. To introduce and evaluate vibration devices, several subcomponents are needed: i) the (mechanical) absorption devices themselves; ii) a control system for active devices; iii) models of the vehicle occupants and their interface with the airframe. All these sub-components are modeled using the notion of *virtual* *feedback loop* in MASST, namely by introducing a state-space subsystem:

$$\dot{\boldsymbol{x}} = \mathbf{A}\boldsymbol{x} + \mathbf{B}\boldsymbol{f} \tag{1a}$$

$$\boldsymbol{y} = \mathbf{C}\boldsymbol{x} + \mathbf{D}\boldsymbol{f} \tag{1b}$$

which is obtained in MASST by assembling the mathematical models of sub-components such as the elastic airframe, the rotors, the actuators etc. Vector $\boldsymbol{x}$ contains the states of the system, which include the coordinates of the base model. The displacements of the points where the absorbers and the human biodynamic models are attached should either be part of the state vector $\boldsymbol{x}$, or need to be expressed as a linear function of the state itself in an effective manner, to accurately represent the force feedback originated from the attached devices or human biodynamics models. Vector $\boldsymbol{y}$ contains the output of the system, which should include both the response of the locations of the performance indicators (for example an occupant seat) and the response of the vibration absorber device attachment positions. The inputs are the loads $\boldsymbol{f}$ at selected nodes of the model, which should include the sources of oscillatory loads ($\boldsymbol{f}_{\mathrm{v}}$) and the loads that result from a modification of the dynamics of the baseline vehicle ($\boldsymbol{f}_{\mathrm{m}}$). The vibratory load excitation vector $\boldsymbol{f}_{\mathrm{v}}$ can contain a broad variety of sources, the most typical ones originating from the main and tail rotors. The modification load vector, $\boldsymbol{f}_{\mathrm{m}}$, is a result of the applied loads at the assembly points of the vibration attenuation devices or human biodynamics models.

MASST interpolates the state-space model in a generic configuration within the corresponding linear models evaluated in the space of prescribed parameters. Thus, MASST guarantees the success of helicopter ride quality assessment as follows:

- flexibility in the source of sub-component formulation;
- high-fidelity overall modeling through sub-component assembly;
- capability of defining sensor-force relations between arbitrary structural points;
- exporting proper models compatible for interaction with vibration devices and human biodynamic models, without the need to reassemble the whole model when the subsystems change.

Therefore, a baseline high-fidelity aeroservoelastic helicopter model prepared in MASST can be extended to include vibration reduction devices, vehicle-human interfaces and human biodynamic models, which is explained next.

### *2.2. Modifying a Baseline Plant*

Evaluation of a vibration attenuation solution often requires the use of several analysis models having distinct characteristics, a large number of iterations for parameter tuning, finding proper locations and simultaneous application of multiple devices. Therefore it is impractical for the vehicle designers to formulate and assemble all the possible vibration attenuation solutions, with a wide range of tuning parameters, within the complete rotorcraft model. Moreover, the total mass of a typical human may not be negligible, compared with that of the vehicle itself; thus, its interaction with the dynamic model of the vehicle is necessary. Last, the mechanical characteristics of a human body change significantly from subject to subject, and biodynamic models show great diversity, which requires exploring a range of biodynamic properties to account for the variability of different population and choosing suitable biomechanical models. Therefore, the cost associated with the assembly of a detailed model of the entire vehicle with the human biodynamic models and vibration attenuation devices is often not affordable with conventional techniques. For this reason, an effective design method could take advantage of a high-fidelity rotorcraft aeroservoelastic modeling platform, which should allow vibration engineers to modify the dynamics of a baseline plant by applying their design changes and human feedback models, but without the need of re-modeling the baseline vehicle.

Vibration attenuation devices and human biodynamic models can be formally modeled in MASST as "controllers", since both produce external force inputs from sensor outputs. The added subsystems can introduce additional states, use a combination of the states of the original system, and contribute to the input of the original system by means of a linear combination of its own original states. This is achieved by defining virtual sensors for motion and loads (forces and moments) at any node of the rotorcraft model's finite element mesh. Accelerations at sensor locations and feedback of the added device can be subsequently extracted from the state space form of the MASST model. The transfer functions for the base model of Eq. (1) are formed as:

$$\boldsymbol{y} = \mathbf{G}\boldsymbol{f} = \left(\mathbf{C}(s\mathbf{I} - \mathbf{A})^{-1}\mathbf{B} + \mathbf{D}\right)\boldsymbol{f} \tag{2}$$

where $s$ is the Laplace variable. Notice that a similar scheme applies to both active and passive vibration attenuation devices. The only difference is that, for the latter, sensors and control forces are intrinsically co-located. The vehicle model must be sufficiently detailed for vibration assessment; therefore, the number of states may typically be of the order of 1000s, or greater. The number of inputs and outputs depend on the relations required to introduce excitation loads and assemble the equivalent mechanical models of human biodynamics and vibration attenuation devices.

To create the feedback path, specific input and output signals are defined in the baseline MASST model. According to Fig. 2:

- the input is defined as the external vibratory loads $\boldsymbol{f}_{\mathrm{v}}$ placed on any appropriate airframe point and/or on the rotors;

- the output $\boldsymbol{y}$ of the virtual helicopter is chosen as the sensors of position, velocity, and acceleration of any airframe point (or rotor point, in multiblade coordinates);

- the modification, either the vibration attenuation device or the human biodynamic model, creates a feedback loop between the sensors corresponding to the motion and the forces exerted ($\boldsymbol{f}_{\mathrm{m}}$) at its attachment points,

  $$\boldsymbol{f}_{\mathrm{m}} = \mathbf{K}_{\mathrm{m}}\boldsymbol{y} \tag{3}$$

  such that $\boldsymbol{f} = \boldsymbol{f}_{\mathrm{v}} - \boldsymbol{f}_{\mathrm{m}}$. The transfer matrix $\mathbf{K}_{\mathrm{m}} = \mathbf{C}_{\mathrm{d}}(s\mathbf{I} - \mathbf{A}_{\mathrm{d}})^{-1}\mathbf{B}_{\mathrm{d}} + \mathbf{D}_{\mathrm{d}}$ represents the synthesis of the device's state-space representation:

  $$\dot{\boldsymbol{x}}_{\mathrm{m}} = \mathbf{A}_{\mathrm{m}}\boldsymbol{x}_{\mathrm{m}} + \mathbf{B}_{\mathrm{m}}\boldsymbol{y} \tag{4a}$$
  $$\boldsymbol{f}_{\mathrm{m}} = \mathbf{C}_{\mathrm{m}}\boldsymbol{x}_{\mathrm{m}} + \mathbf{D}_{\mathrm{m}}\boldsymbol{y} \tag{4b}$$

  in which vector $\boldsymbol{x}_{\mathrm{m}}$ contains the (possibly hidden) internal state of the device or human biodynamic model.

The inner complexity of the vibration attenuation device or human biodynamics model is arbitrary, as long as the connections to the vehicle are

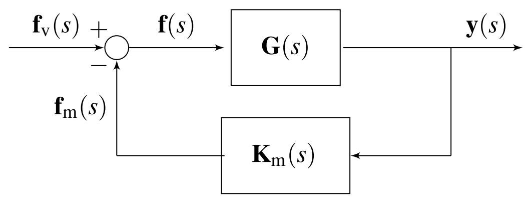


Figure 2: Block diagram representation of the vehicle ($\mathbf{G}$) and of the modification that introduces the dynamics of the human body or of a vibration attenuation device ($\mathbf{K}_{\mathrm{m}}$).

properly defined. Hence, the matrices can be obtained using simple lumped element models or sophisticated tools such as finite elements or multibody dynamics. Regardless of the dimension of the matrices, the response of the modified system is obtained as a function of the vibratory loads $\boldsymbol{f}_{\mathrm{v}}$:

$$\boldsymbol{y} = (\mathbf{I} + \mathbf{G}\mathbf{K}_{\mathrm{m}})^{-1}\,\mathbf{G}\boldsymbol{f}_{\mathrm{v}} \tag{5}$$

Since $\mathbf{G}$ is the result of a high fidelity tool with an arbitrarily large number of states, inputs and outputs, the gain matrix $\mathbf{K}_{\mathrm{m}}$ can easily be defined using force-response relations of the attached device or human vibration model. As a result, the proposed method supports the decoupling of vehicle design and vibration analysis, whilst providing coordination through a common platform. Thus, the two processes can be accelerated, the assembly cost can be reduced, and the vibration attenuation solutions can be easily integrated as the design evolves.

### *2.3. Processing Vibration Signals*

When the baseline model is extended with human biodynamic models and vibration reduction devices, the accelerations can be calculated for a measured or computed set of vibratory loads at selected flight conditions and vehicle configurations. However, as recommended by ISO-2631, these accelerations should further be root-mean-square (RMS) averaged and scaled using frequency-weights. An important factor in using RMS averaging is the modulus of the ratio of the maximum instantaneous peak value of the acceleration signal to its RMS value, i.e. the crest factor. A crest factors of 9 is used as a threshold for the reliability of RMS averaging [30]. This limit is satisfied if $N_b$/rev harmonic vibrations are considered, which have a crest factor of $\sqrt{2} \approx 1.4$. Moreover, the measurement or computation should be made at the interface between the subject and the airframe, which typically refers to the calculation of the translational accelerations along three axes at the seat surface:

$$\boldsymbol{a}(t) = \begin{bmatrix} a_x(t) & a_y(t) & a_z(t) \end{bmatrix}^T \tag{6}$$

as a function of time $t$. However, since frequency weighting cannot be applied to a signal in the time domain, the Fourier series expansion ($\mathfrak{F}$) is performed:

$$\mathfrak{F}\left(\begin{bmatrix} a_x(t) \\ a_y(t) \\ a_z(t) \end{bmatrix}\right) = \sum_{n=-\infty}^{n=\infty} \begin{bmatrix} A_x(\omega_n) \\ A_y(\omega_n) \\ A_z(\omega_n) \end{bmatrix} e^{\mathrm{j}\omega_n t} \tag{7}$$

where $A_{x,y,z}$ are the accelerations in the frequency domain. Then, after applying frequency and direction weights, the frequency weighted acceleration in time domain becomes:

$$\boldsymbol{a}_w(t) = \sum_{n=-\infty}^{n=\infty} \begin{bmatrix} W_d(\omega_n) k_x A_x(\omega_n) \\ W_d(\omega_n) k_y A_y(\omega_n) \\ W_k(\omega_n) k_z A_z(\omega_n) \end{bmatrix} e^{\mathrm{j}\omega_n t} \tag{8}$$

The ratings are given in terms of RMS magnitude of the weighted acceleration over the exposure time $T$:

$$a_{w,\mathrm{RMS}} = \sqrt{\frac{1}{T}\int_0^T \boldsymbol{a}_w^T \boldsymbol{a}_w dt} \tag{9}$$

In case of $N_b$ /rev dominant single frequency, the weighted acceleration becomes:

$$a_{w,\mathrm{RMS}} = \frac{1}{\sqrt{2}}\sqrt{(W_d k_x A_{x,N_b})^2 + (W_d k_y A_{y,N_b})^2 + (W_k k_z A_{z,N_b})^2} \tag{10}$$

### *2.4. Comfort Rating*

After the combined model is analyzed and accelerations at the human-vehicle interface surfaces are obtained, the effect of vibration attenuation solutions on ride quality can be evaluated using individual and overall comfort rating.

Table 2: Comfort rating after ISO-2631 (Section C.2.3), converted to $g$ at sea level.

| | |
|---|---|
| Less than 0.03 $g$ | not uncomfortable |
| 0.03 $g$ to 0.06 $g$ | not comfortable |
| 0.05 $g$ to 0.10 $g$ | a little uncomfortable |
| 0.08 $g$ to 0.16 $g$ | fairly uncomfortable |
| 0.13 $g$ to 0.25 $g$ | uncomfortable |
| Greater than 0.20 $g$ | very uncomfortable |

### *2.4.1. Individual Occupant Rating*

Given the averaged weighted magnitude of acceleration ($a_{w,\mathrm{RMS}}$ of Eq. (9)), ISO-2631 suggests a qualitative scale, as presented in Table 2. The effect of a vibration attenuation device can simply be evaluated by comparing the qualitative levels.

Another criterion is the quantitative Vibration Dose Value (VDV), which takes the time of exposure into account:

$$\mathrm{VDV} = \left[\int_0^T [\bar{a}_w(t)]^4 \mathrm{d}t\right]^{\frac{1}{4}} \tag{11}$$

where $\bar{a}_w(t) = \sqrt{\boldsymbol{a}_w(t)^T \boldsymbol{a}_w(t)}$ is the magnitude of the instantaneous frequency weighted acceleration and $T$ is the total exposure time. Eq. (11) requires the duration of flight to calculate the VDV. Without loss in generality, a relative change can be formulated for $N_b$/rev vibrations and help engineers to compare the benefits of adding a vibration device. For the same time of exposure, the effect can be evaluated as:

$$\mathrm{VDV}_{\mathrm{rel}} = \frac{\mathrm{VDV}}{\mathrm{VDV}_0} = \frac{\left[\int_0^T [\bar{a}_w(t)]^4 \mathrm{d}t\right]^{\frac{1}{4}}}{\left[\int_0^T [\bar{a}_{w,0}(t)]^4 \mathrm{d}t\right]^{\frac{1}{4}}} \tag{12}$$

where subscript $(\bullet)_0$ refers to the nominal plant without any vibration attenuation device. In case of harmonic response at a dominant frequency, the time-averaged and time-integrated vibration comfort criteria give the same amount of relative improvement:

$$\mathrm{VDV}_{\mathrm{rel}} = \frac{A_w(N_b\Omega)}{A_{w,0}(N_b\Omega)} \tag{13}$$

since VDV $= 0.7825\, A_w \sqrt[4]{T}$ for predominantly harmonic signal with amplitude $A_w$ and exposure time $T$ [34].

*2.4.2. Overall Rating*

A successful vibration attenuation solution is expected to result in a cabin response that is less sensitive to the number of occupants and their distribution, which can play a non-trivial role in transportation class helicopters, since the weight of each passenger is not always negligible and can affect the overall vibration distribution. This cannot be fully understood from individual rating alone, hence defining the most and least comfortable seating distribution as the number of passenger changes can help a complete evaluation of the vibration attenuation solution. To compare the sensitivity of vibrations to seating configuration, a performance index is formulated. First, given the number of passengers ($n_p$) for a total $N_s$ number of seats, the possible number of seating configurations is given as a combination function:

$$\mathrm{PS}(N_s, n_p) = \mathrm{C}(N_s, n_p) = \binom{N_s}{n_p} = \frac{N_s!}{(N_s - n_p)!n_p!} \tag{14}$$

where the passenger number $n_p$ is varied from 0 to $N_s$. Then, a vector of the RMS magnitudes of frequency weighted accelerations at $N_s + 2$ locations are defined (the two pilots are always present):

$$\boldsymbol{y} = [a_{\mathrm{CKPT1}}\ \ a_{\mathrm{CKPT2}}\ \ a_{\mathrm{CBN1R}}\ \ a_{\mathrm{CBN1L}}\ \ \ldots\ \ a_{\mathrm{CBN4R}}\ \ a_{\mathrm{CBN4L}}]^T \tag{15}$$

Now, a performance index (PI) is defined as the normalized square root of a quadratic matrix multiplication:

$$\mathrm{PI} = \frac{\sqrt{\boldsymbol{y}^T \mathbf{W} \boldsymbol{y}}}{n_p + 2} \tag{16}$$

where the division by $n_p{+}2$ is added to normalize the performance index with the number of occupied seats. The diagonal weight matrix $\mathbf{W}$ has elements equal to 1 for occupied seats and 0 for the empty ones. The PI is evaluated for all possible seating sequences, and the most and the least comfortable configurations are obtained.

## 3. Application

This section presents how a typical model is built for the evaluation of vibration reduction solutions using the proposed framework.

### *3.1. Baseline Helicopter Model*

The analyses are based on data representative of a generic, medium weight helicopter with a 5 blade main rotor as shown in Fig. 3(a). The state-space model includes:

- the 6 airframe rigid body dynamics;
- the airframe stability derivatives, calculated from the aerodynamic look-up tables of the fuselage, horizontal tail and vertical tail in CAMRAD/JA (a comprehensive rotorcraft analysis software [35]), necessary to capture the low-frequency flight mechanics behavior of the helicopter;
- elastic bending and torsion modes of the airframe up to a frequency range of 50 Hz, extracted from a detailed finite element model in NASTRAN (a popular Finite Element solver), which is characterized by more than 30000 nodes and 17000 elements including beams, shells and solids;
- main and tail aeroelastic rotors, modeled in CAMRAD/JA and characterized by two bending modes (the first in lead-lag and the second in flap, typical of soft in-plane articulated rotors) plus one torsion mode (related to the control chain compliance), in multiblade coordinates. The main rotor also includes the Pitt-Peters (Ref. [36]) axial inflow state;
- transfer functions of main and tail rotor servoactuators, formulated in Matlab/Simulink, considering the servo-valve and the dynamic compliance [37]. A gear ratio matrix is therefore used to convert the linear actuator displacements into collective and cyclic commands;
- the nodes and coordinates for the sensors (Fig. 3(b)) and the forces, directly defined in MASST with the number of evenly distributed passenger seats set to $N_s = 8$, considering the space available in the cabin;
- structural damping can change the accelerations at the sensors. MASST can superimpose proportional damping over a helicopter model, which is a standard process to consider structural damping. However, no airframe structural damping was added, since experimental data were not available at this stage.

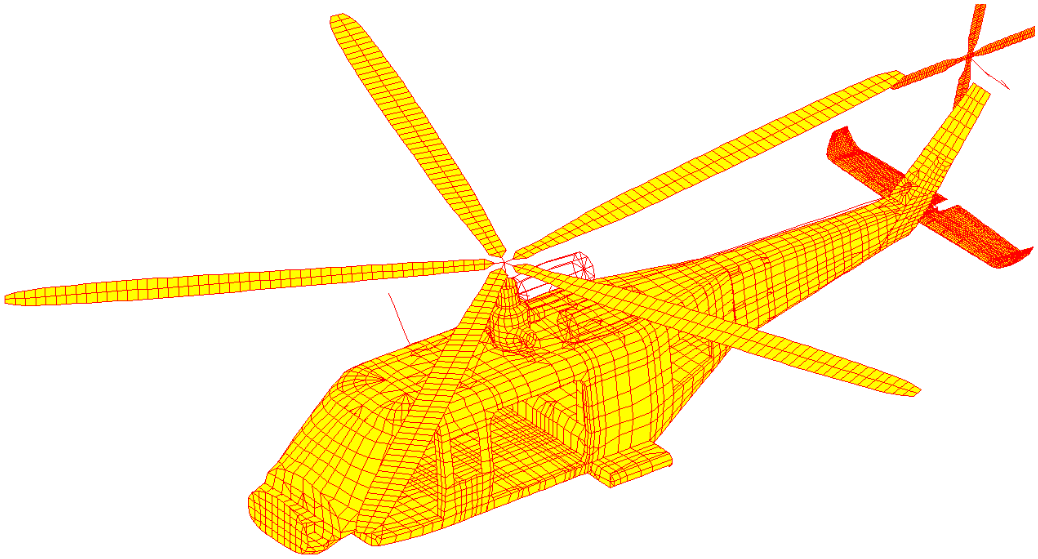

(a) MASST model

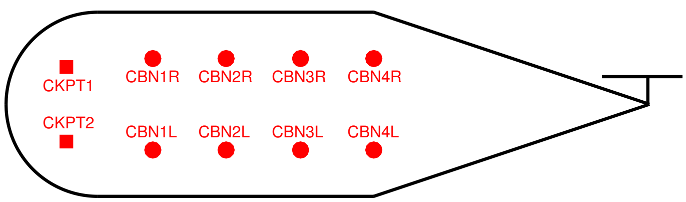


(b) Sensors

Figure 3: MASST helicopter model (a) and sensor locations (b): cockpit (CKPT), cabin (CBN), left (L) and right (R).

### *3.2. Identification of Hub Force*

The comfort assessment requires the knowledge of the oscillatory loads, which can be determined either by numerical simulation or experimental campaign. The main rotor is considered as the source of vibratory loads, although an arbitrary number of external loads can be handled by the proposed method. Measured values representative of the axial elongations of the gearbox suspension struts of a helicopter of medium-weight class at typical $N_b\Omega \approx 25$ Hz are used. Among available data for different flight conditions, the case with the largest amplitude $N_b\Omega$ loads has been used as the most critical condition. The resulting forces, with the numerical values reported in Table 3, are applied on the main rotor hub of the model.

Table 3: Maximum estimated hub force components at $N_b$/rev frequency relative to take-off weight (TOW). The phase of the excitation force was not available, thus it was assumed to be zero.

| Component | Amplitude (% TOW) | Phase (deg.) |
|---|---|---|
| Longitudinal | 3.6 | 0 |
| Lateral | 1.4 | 0 |
| Vertical | 16.4 | 0 |

### *3.3. Human-Seat Vibration Model*

In ISO-2631, accelerations are measured at the interface between the occupant and the vehicle. No matter how complex, a connection between the occupant and the cabin floor usually exists, which modifies the level of excitation transferred to the occupant's body. In turn, the interface between the structure and human biomechanics feeds loads back to the airframe. This interaction of the vehicle with the interface-human system might affect the magnitude of the accelerations. Furthermore, the accumulation of these modifications to the system might alter the overall comfort level as the number of occupants increases. In the present case, for example, the total mass of the vehicle changes by more than 10% between the no-occupant and the full occupancy configurations at maximum takeoff weight (MTOW). Therefore, the dynamic interaction of the human body with the vehicle should not be ignored in comfort rating analysis.

Although the proposed method can handle models of increasing complexity originating from different sources, lumped human and seat models are considered here, to provide a sufficiently accurate and generalized infrastructure for vibration rating. This is a reasonable choice, since using complex biodynamic modeling techniques do not result in significant difference in rotorcraft comfort assessment [40]. That of Wan and Schimmels [38] is a classical four degree of freedom lumped model of human body for vibration comfort, in which linear springs and dampers idealize the connections between the body parts (see Ref. [41] for a comparison of 4 degrees of freedom lumped models). The seat is described as a mass suspended by a spring and damper, whereas the cushion is a massless spring-damper; both are adapted from a helicopter application [39]. The combined seat-human system, as illustrated in Fig. 4, is excited through the seat support by the floor motion, $z_f$. The coupled equations of the combined human-seat-cushion system are cast in the form of Eq. (4) and added to the baseline helicopter model. Each

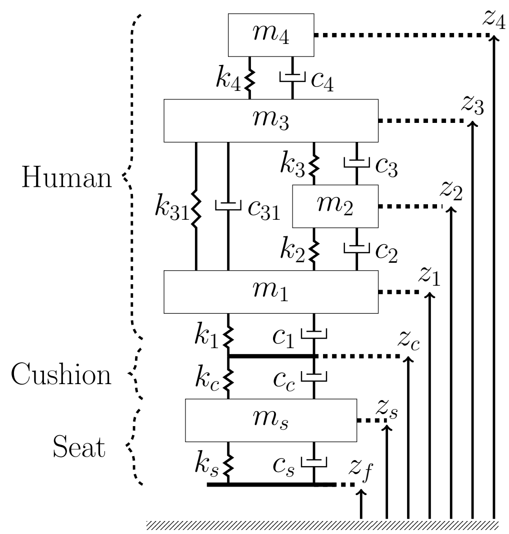


Figure 4: Modified Wan-Schimmels of lumped human model [38], seated on a cushion supported by a seat model (from [39]).

occupant with the seat adds 10 additional states $\boldsymbol{x}_{\mathrm{m}}$ to the baseline system within the $\mathbf{K}_{\mathrm{m}}$ feedback of Fig. 2. The numerical values of the parameters are reported in Table 4.

Table 4: Numerical values for the Wan-Schimmels Model [38] and seat-cushion model [39].

| Component | Index | $m_i$ (kg) | $c_i$ ( $\mathrm{N\,s\,m^{-1}}$) | $k_i$ ($\mathrm{N\,m^{-1}}$) |
|---|---|---|---|---|
| Abdomen | i=1 | 36.00 | 2475.00 | 49341.60 |
| Bowels | i=2 | 5.50 | 330.00 | 20000.00 |
| Chest | i=3 | 15.00 | 200.00 | 10000.00 |
| Head | i=4 | 4.17 | 250.00 | 134400.00 |
| Spine | i=31 | - | 909.09 | 192000.00 |
| Seat | i=s | 13.5 | 750.00 | 22600.00 |
| Cushion | i=c | - | 159.00 | 37700.00 |

### *3.4. Vibration Reduction Devices*

The coupled helicopter-occupant model is extended using typical passive absorbers to illustrate the method, without excessive loss of generality. The corresponding devices are sketched in Fig. 5 at their typical locations. The individual and overall comfort ratings are calculated and compared with those of the baseline for three configurations.

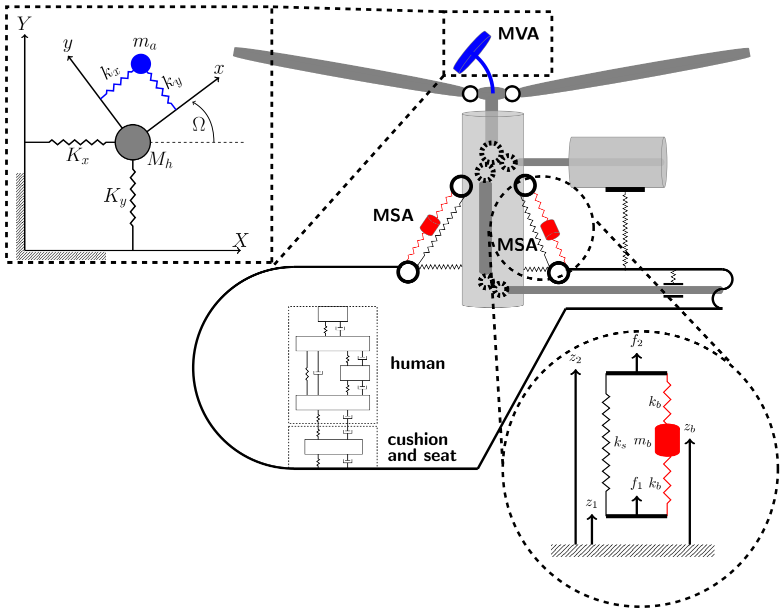


Figure 5: Illustrative vibration attenuation devices and an occupant at their typical locations.

1. The first one considers the isolation of the fuselage from the gearbox using axial spring mass absorbers (MSA). Each resonator is attached in parallel with the corresponding gearbox strut, as shown in Fig. 5. The spring without mass ($k_s$) is the original strut, whereas the tuning mass ($m_b$) connected to the same terminals of the original strut by two identical springs ($k_b$) represents the MSA. The nominal tuning frequency for the isolation of the fuselage side is:

$$\omega = \sqrt{\left(2 + \frac{k_b}{k_s}\right) \frac{k_b}{m_b}} \tag{17}$$

2. The second configuration is a Mast Vibration Absorber (MVA), which aims at reducing in-plane vibrations transmitted by the rotor mast to the gearbox and airframe [42]. A mass $m_a$ is mounted on the rotor head via an elastic beam whose flexural rigidity is modeled by linear springs $k_x, k_y$, as sketched in Fig. 5. The equivalent hub mass $M_h$ moves in an inertial frame $(X, Y)$ and it is connected to the gearbox by equivalent springs of stiffness $K_x$ and $K_y$. The MVA mass, $m_a$, in the rotating

frame $(x, y)$, rotates with the mast at the rotor angular speed $\Omega$. The flexural stiffness of the beam is modeled as springs of stiffness $k_x$ and $k_y$. In case of equal spring stiffness, $k_x = k_y = k_a$, the isolation frequency of hub in-plane vibrations is:

$$\omega = \sqrt{\frac{k_a}{m_a}} \tag{18}$$

3. The third configuration illustrates an interesting feature of a modular high-fidelity vibration analysis tool: the capability to simultaneously consider independent solutions. For this purpose, both the MSA and MVA devices are mounted on the same plant. The equations of both vibration devices are cast in the form of Eq. (4) and added to the baseline helicopter model.

## 4. Results and Discussion

This section presents the comfort ratings of individual seating positions and illustrates the effect of the number of passengers and their seating distributions using the models and criteria defined in the previous section. It should be noted that verification of the numerical model through flight or ground tests were not performed. Thus, deviations from the real behaviour could exist. The following applications predict changes in vibration level achieved with respect to the baseline model for illustrative purposes, and should not be interpreted as the actual means of vibration reduction of a particular helicopter. Therefore, the results are presented in either qualitative scale or in relative value with respect to the baseline.

### *4.1. Comfort Rating of Individual Seating Positions*

The human biodynamic model is coupled to the helicopter model through seats for the 10 seating positions. The performance of each position is evaluated for the fully occupied helicopter. Fig. 6 presents the individual ratings of the three configurations and compare the results with those of the baseline. Both qualitative and relative VDV forms are used, although one form can be sufficient if vibration is predominantly harmonic. Fig. 6(a) shows the relative change in vibration dose value and the time-averaged rating before and after the application of the mass-spring absorber on the struts. Similarly, Fig. 6(b) gives the performance of the MVA device. For both cases, improvement and degradation occur at individual seats. The MSA is successful in overall vibration performance improvement. On the other hand, if MVA is the sole vibration attenuation device, it might fail to improve the overall ride quality at some seating positions. This failure is attributed to the relatively low magnitude of in-plane hub forces, as reported in Table 3 for the target helicopter, and lower human vibration sensitivity along in-plane directions, as one can infer from the value of $W_d$ in Fig. 1 near 25 Hz.

Fig. 6(a) and Fig. 6(b) suggest that the simultaneous application of multiple devices instead of a single device might have an overall beneficial effect with respect to all components of accelerations resulting from hub loads simultaneously acting in all directions. The upper plot of Fig. 6(c) shows the relative change in VDV, which results in significant reductions throughout all sensor locations. The lower plot of Fig. 6(c) presents the instantaneous rating before and after the application of the MSA in parallel with the struts and of the MVA on the rotor mast. The comfort of all seats was to the best possible rating of ISO-2631. The combined performance is found to be better than the sum of the individual performances of the two devices. When implemented alone, a single device can amplify some elastic airframe modes, which reduces the benefits. The undesired amplifications caused by the application of a single device can be reduced using multiple devices. Therefore, the simultaneous application of two or more device types with different aims can collaborate to considerably reduce the level of vibration perception in the cockpit and cabin. This can also help engineers in optimizing the response at the cost of adding mass.

### *4.2. Overall Rating*

The effect of the seating configuration is analyzed in terms of the maximum and minimum value of the performance index as a function of the passengers for all three configurations and the baseline plant. The human biodynamic model is only added for occupied seats, while the mechanical seat model is preserved regardless of the cabin seat occupation. Fig. 7 presents the dimensional maxima and minima of the performance index as a function of the number of passengers. Note that since there is only one possible seating distribution for both an empty and a fully occupied plant, the function is single-valued. The minima and maxima of Fig. 7 correspond to specific seating distributions. Based on the value of the performance index of the four configurations, Fig. 8 shows the most and the least comfortable seating distributions as functions of the number of passengers. The empty and fully occupied seating distributions are trivial; thus, they are not included. It is

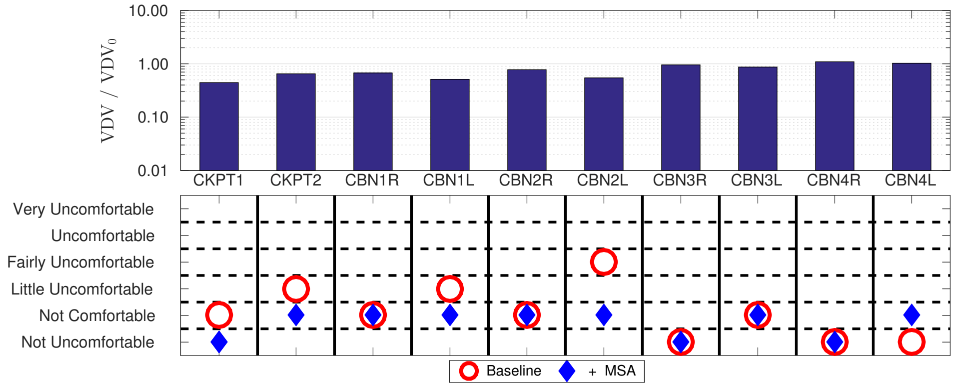


(a) Mass Spring Absorber (MSA)

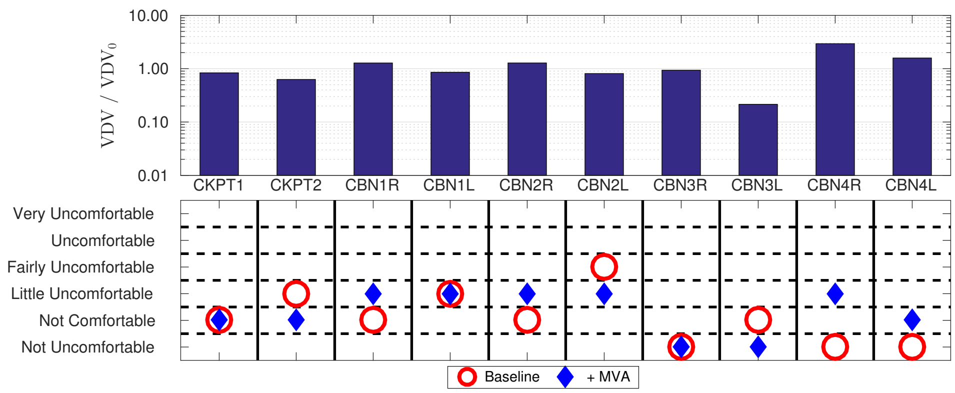


(b) Mast Vibration Absorber (MVA)

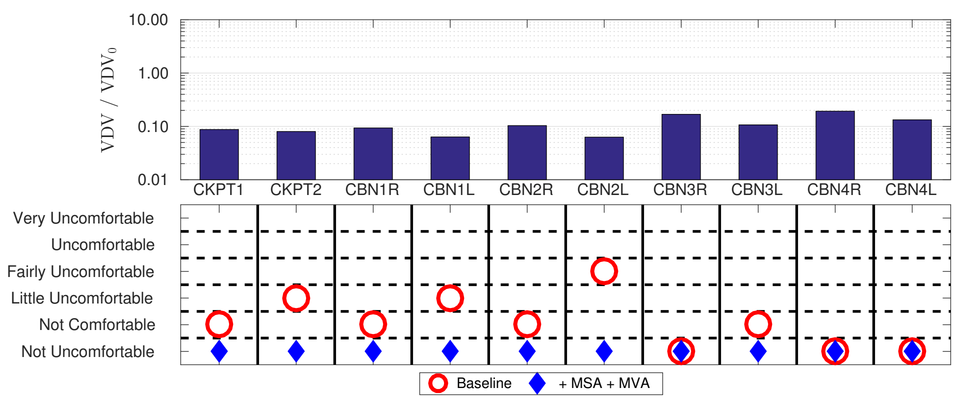


(c) Simultaneous Application of MSA and MVA

Figure 6: Performance of vibration devices for three different solutions, each includes Relative Vibration Dose Value and time-averaged qualitative rating.

worth noticing that no obvious pattern appears for the seating distributions, such as starting from the first or last row. This suggests that the distribution of passengers in specific seating places can affect the vibration rating; thus, they need to be taken into account in ride quality assessment. Moreover, the addition of the occupants changes the overall vibration rating significantly, therefore justifying the coupled analysis of helicopter and human biodynamics for comfort reduction.

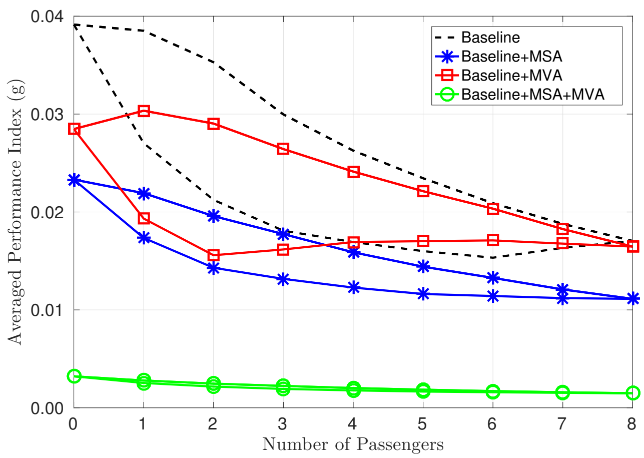


Figure 7: The effect of seating distribution on the dimensional performance index, averaged with the number of occupied seats. Baseline: helicopter model and two pilots; MSA: mass spring absorber on struts; MVA: mast vibration absorber.

## 5. Conclusions

A virtual environment for helicopter ride quality assessment and an effective tool for incorporating arbitrary vibration reduction devices and human biodynamic models is presented. In brief:

- MASST is a high-fidelity state-space aeroservoelastic analysis environment in which sub-components, originally modeled in their most natural modeling and analysis environments, are assembled;
- MASST enables a vibration engineer to receive high-fidelity nominal plant state-space matrices and work on the vibration attenuation solutions without spoiling the nominal model;

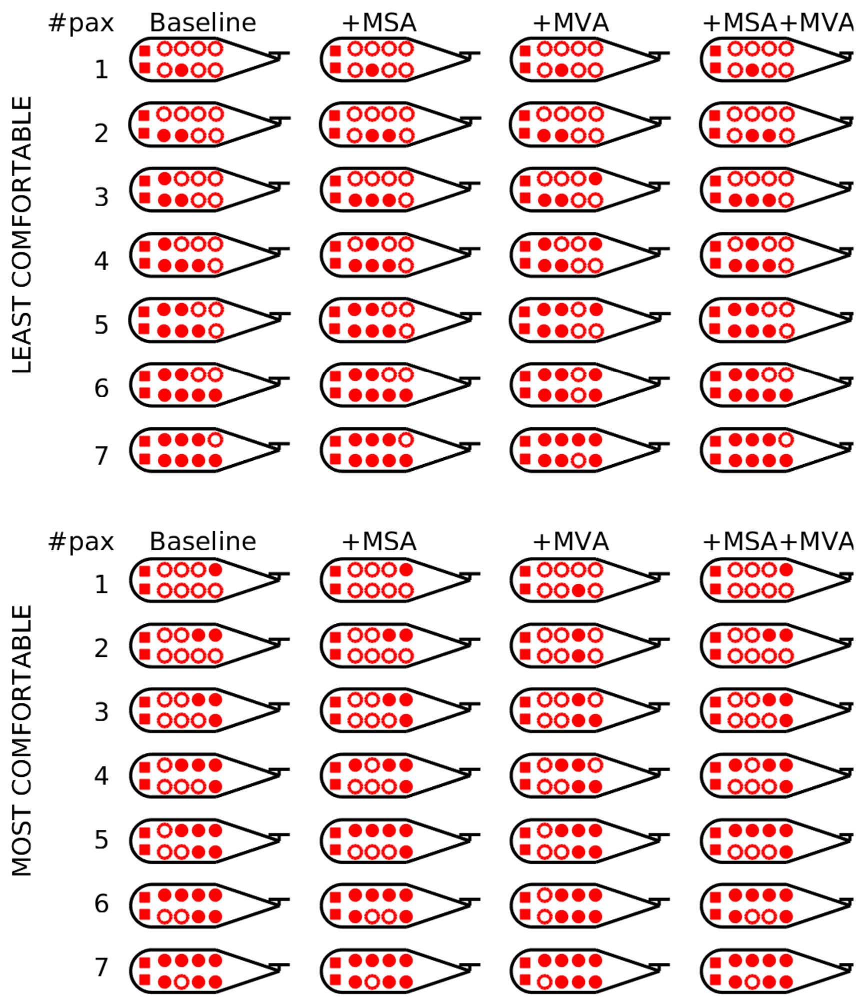


Figure 8: The most and least comfortable seating configurations as functions of the number of passengers which allow multiple seating configurations.

- the vibration reduction solutions and human biodynamic models are added in form of generalized feedback controllers. The related input-output channels must be previously defined in the nominal model;
- sensors and external forces can be defined at any location of the nominal model, allowing a detailed formulation of the vibration reduction objective function;
- an arbitrary number of vibration reduction solutions can be evaluated

simultaneously, thus allowing the estimation of their combined effect and the definition of an accurate cost function.

The method is illustrated using three vibration reduction solutions: (a) axial mass-spring absorbers parallel to each of the main gearbox suspension struts, focusing on vertical loads, and (b) a mast vibration absorber mounted on the rotor head, focusing on in-plane loads, and (c) the simultaneous application of both. Based on the results obtained using the proposed modular high-fidelity simulation tool MASST, the following recommendations are made for an accurate evaluation of vibration reduction solutions:

- for an effective vibration attenuation solution, it is worth considering the simultaneous application of two or more independent devices, focusing on independent loads absorption;
- the biodynamics of the occupants, and the passenger distribution over the cabin seats can significantly affect the overall performance index, thus future considerations of helicopter design to meet ride quality standards should consider this fact;
- an effective vibration attenuation solution should induce less variability in the performance index for different passenger numbers and arrangements.

**Acknowledgements**

This work received partial support by Leonardo Helicopter Division. The authors particularly acknowledge LHD for providing part of the data used in the analysis.

**References**

[1] K. L. Harrer, D. Yniguez, M. M. Maria, D. Ellenbecker, N. Estrada, M. Geiger, Whole body vibration exposure for MH-60s pilots, in: 43th SAFE, Utah, USA.

[2] K. S. Brentner, F. Farassat, Modeling aerodynamically generated sound of helicopter rotors, Progress in Aerospace Sciences 39 (2003) 83 – 120.

[3] R. L. Bielawa, Rotary Wing Structural Dynamics and Aeroelasticity, AIAA, Washington, DC, 2nd edition, 2005.

[4] T. Rath, W. Fichter, A closer look at the impact of helicopter vibrations on ride quality, in: AHS 73rd Annual Forum, Forth Worth, TA, USA.

[5] W. Johnson, Rotorcraft Aeromechanics, Cambridge University Press, New York, 2013.

[6] R. Desjardins, W. Hooper, Rotor lsolation of the hingeless rotor BO-105 and YUH-61 helicopters, in: 2nd European Rotorcraft and Powered Lift Aircraft Forum.

[7] R. Desjardins, W. Hooper, Antiresonance rotor isolation for vibration reduction, in: American Helicopter Society 34th Annual Forum, Washington DC.

[8] D. Braun, Development of antiresonance force isolators for helicopter vibration reduction, in: 6th European Rotorcraft Forum, Bristol, UK.

[9] P. Hege, G. Genoux, The SARIB vibration absorber, in: 9th European Rotorcraft and Powered Lift Aircraft Forum.

[10] D. Halmes, LIVE liquid inertia vibration eliminator, in: American Helicopter Society 36th Annual Forum, Washington DC.

[11] D. Halwes, Total main rotor isolation system, in: American Helicopter Society Northeast Region Specialist Meeting on Helicopter Vibration, Hartford, CT.

[12] D. Halwes, Total Main Rotor Isolation System Analysis, CR NAS1-16211, NASA, 1981.

[13] D. P. McGuire, Active vibration control using fluidlastic pylon struts, in: American Helicopter Society 62nd Annual Forum, Phoenix, Arizona (USA).

[14] M. . Hamouda, G. Pierce, Helicopter vibration suppression using simple pendulum absorbers on the rotor blade, CR NSG-1592, NASA, 1982.

[15] R. W. White, A fixed frequency rotor head vibration absorber based upon G.F.R.P. springs, in: 5th European Rotorcraft Forum, Amsterdam, Netherlands.

[16] Y. Chen, U. S. Yapa, A. Price, V. Wickramasinghe, Evaluation of aircrew whole-body vibration and mitigation solutions for helicopter flight engineers, in: AHS 73rd Annual Forum, Forth Worth, TA, USA.

[17] J. T. Pearson, R. M. Goodall, I. Lyndon, Active control of helicopter vibration, Computing & Control Engineering Journal 5 (1994) 277–284. doi:10.1049/ccej:19940608.

[18] G. Lehmann, The effect of higher harmonic control (hhc) on a four-bladed hingeless model rotor, Vertica 9 (1985) 273–284.

[19] C. Kessler, Active rotor control for helicopters: motivation and survey on higher harmonic control, CEAS Aeronaut. J. available online (2011). doi:10.1007/s13272-011-0005-9.

[20] N. D. Ham, B. L. Behal, M. Robert M., Jr, Helicopter rotor lag damping augmentation through individual-blade-control, Vertica 7 (1983) 361–371.

[21] N. D. Ham, Helicopter individual-blade-control research at MIT 1977–1985, Vertica 11 (1987) 109–122.

[22] C. Kessler, Active rotor control for helicopters: individual blade control and swashplateless rotor designs, CEAS Aeronaut. J. available online (2011). doi:10.1007/s13272-011-0001-0.

[23] M. Gennaretti, M. Molica Colella, G. Bernardini, Prediction of tiltrotor vibratory loads with inclusion of wing-proprotor aerodynamic interaction, Journal of Aircraft 47 (2010) 71–79. doi:10.2514/1.41825.

[24] C. Fuller, S. Elliott, P. Nelson, Active Control of Vibration, Academic Press, 1996.

[25] T. Krysinski, D. Ferullo, A. Roure, Helicopter vibration control methodology and flight test validation of a self-adaptive anti-vibration system, in: 24th European Rotorcraft Forum, Marseille, FR.

[26] ISO, ISO MEchanical vibration and shock - Evaluation of human exposure to whole-body vibration, Technical Report ISO2631-1, ISO, 1997.

[27] J. D. Leatherwood, S. A. Clevenson, A design tool for estimating passenger ride discomfort within complex ride environments, The Journal of the Human Factors and Ergonomics Society 22 (1980) 291–312.

[28] AMCOM, Requirements for Rotorcraft Vibration Specifications, Modeling and Testing, ADS-27A, US Army AMCOM, 2006.

[29] A. H. Law, H. E. W. Beatty, J. Keillor, V. Wickramasinghe, Pilot head and neck response to helicopter whole body vibration and head-supported mass, in: AHS 73rd Annual Forum, Forth Worth, TA, USA.

[30] N. Mansfield, Human Response to Vibration, Taylor & Francis, 2004.

[31] P. Masarati, V. Muscarello, G. Quaranta, Linearized aeroservoelastic analysis of rotary-wing aircraft, in: 36th European Rotorcraft Forum, Paris, France, pp. 099.1–10.

[32] P. Masarati, V. Muscarello, G. Quaranta, A. Locatelli, D. Mangone, L. Riviello, L. Viganò, An integrated environment for helicopter aeroservoelastic analysis: the ground resonance case, in: 37th European Rotorcraft Forum, Gallarate, Italy, pp. 177.1–12.

[33] R. R. Craig, Jr., M. C. C. Bampton, Coupling of substructures for dynamic analysis, AIAA Journal 6 (1968) 1313–1319.

[34] M. J. Griffin, Handbook of Human Vibration, Academic Press, London, 1990.

[35] W. Johnson, CAMRAD/JA, A Comprehensive Analytical Model of Rotorcraft Aerodynamics and Dynamics, Johnson Aeronautics Version, Johnson Aeronautics, 1988.

[36] D. M. Pitt, D. A. Peters, Theoretical prediction of dynamic-inflow derivatives, Vertica 5 (1981) 21–34.

[37] H. E. Merritt, Hydraulic Control Systems, John Wiley & Sons, New York, 1967.

[38] Y. Wan, J. M. Schimmels, Optimal seat suspension design based on minimum simulated subjective response, Journal of biomechanical engineering 119 (1997) 409–416.

[39] Y.-T. Choi, N. Wereley, Biodynamic response mitigation to shock loads using magnetorheological helicopter crew seat suspensions, Journal of Aircraft 42 (2005) 1288.

[40] A. Tamer, A. Zanoni, V. Muscarello, A. Cocco, G. Quaranta, P. Masarati, Biodynamic modeling techniques for rotorcraft comfort evaluation, Aerotecnica Missili & Spazio (2019).

[41] X.-X. Bai, S.-X. Xu, W. Cheng, L.-J. Qian, On 4-degree-of-freedom biodynamic models of seated occupants: Lumped-parameter modeling, Journal of Sound and Vibration 402 (2017) 122 – 141.

[42] T. Krysinski, F. Malburet, Mechanical Vibrations, ISTE Ltd, 2007.